

# Aluminum Solid-Solution Coating for High-Temperature Corrosion Protection

Alina Agüero<sup>1</sup> · Marcos Gutiérrez<sup>1</sup> · Raúl Muelas<sup>2</sup>

Received: 12 December 2016 / Published online: 12 January 2017  
© Springer Science+Business Media New York 2017

**Abstract** Iron aluminide coatings are very resistant to corrosion at 600–700 °C. However, interdiffusion is responsible for a significant reduction of the Al content at the coating surface. A stable diffusion barrier could in principle prevent this degradation mechanism. A new diffusion barrier based on nitrogen was produced and was very effective in reducing coating–substrate interdiffusion on P92. After nitriding P92, an Al slurry was applied and heat-treated, resulting in an overlay coating consisting of an Al solid solution with Cr and Fe. This coating was thinner and quite different from the several Al–Fe intermetallics obtained without nitriding and was fully characterized. A diffusion study was conducted and the results showed that after 2000 h at 650 °C, the new coating suffered very little changes and no interdiffusion with the substrate in contrast with the intermetallic coating deposited without nitriding. Testing under steam and fire-side atmospheres showed promising behavior.

**Keywords** Aluminum solid solution coating · High-temperature corrosion · Diffusion barrier · Nitriding

---

✉ Marcos Gutiérrez  
gutierrezdom@inta.es

Alina Agüero  
agueroba@inta.es

Raúl Muelas  
modsurf3.pers\_externo@inta.es

<sup>1</sup> Instituto Nacional de Técnica Aeroespacial, Ctra. Ajalvir Km 4, 28850 Torrejón de Ardoz, Spain

<sup>2</sup> Ingeniería y Sistemas para la Defensa de España, Madrid, Spain

## Introduction

Diffusion aluminide coatings are widely used to protect Fe [1], Ni [2], Co [3], Ti [4], and Mg [5]-based alloys from high-temperature oxidation or environmental corrosion. At high temperature, the protection conferred by these coatings is based on their capability of forming an adherent, dense, and stable  $\text{Al}_2\text{O}_3$  layer, and one of the main degradation mechanisms of these coatings is the loss of Al by coating–substrate interdiffusion [6, 7]. Moreover, interdiffusion causes Kirkendall porosity and in many cases the formation of a diffusion zone between the coating and the substrate which may contain brittle phases in the base alloy [8]. On the other hand, some alloying elements including Ti, Mo, and W present in the substrate may diffuse outwards and weaken the adhesion of the protective oxide to the substrate [9]. The basic diffusion mechanism which is responsible for the processes are thermally induced volume and grain boundary diffusion.

Important efforts have been undertaken in order to prevent or reduce interdiffusion by applying barriers such as Re–Ni [10], Ta–Ir [11], Hf–Ni, Hf–Pt [12], Ni– $\text{CeO}_2$  [13], and  $\text{Al}_2\text{O}_3$  [14] mostly by electroplating or sputtering on Ni-base alloys prior to applying overlay MCrAlY coatings, or to aluminizing by pack cementation or CVD. However, to use a diffusion barrier on a diffusion aluminide coating may seem as a contradiction, as the concept of this type of coatings is based on the formation of intermetallic phased by interdiffusion of added aluminum with the elements present in the substrate. Examples of these phases are  $\text{Ni}_2\text{Al}_3$  and NiAl on Ni base alloys and  $\text{Fe}_2\text{Al}_5$  and FeAl on steels. If the diffusion is totally blocked, the coating will not be formed. Ideally, a diffusion barrier for this type of protective systems must allow the formation of a stable coating, and then stop or retard further interactions with the substrate.

In particular, Fe aluminides applied on ferritic/martensitic steels have shown to be very resistant to corrosion under steam, combustion atmospheres, and air at 600–700 °C [15–17]. However, interdiffusion is responsible for a significant reduction of the Al content at the coating surface, as well as for the formation of AlN acicular precipitates when the steel contains enough nitrogen. Nitrogen is added to steels for strengthening purposes and its loss due to precipitation of AlN can be detrimental to the steels' mechanical properties. A stable diffusion barrier could in principle prevent these two degradation mechanisms.

Recently, Rouaix-Vande Put and Pint [18] observed that ODS ferritic alloys containing N could not be aluminized by CVD due to the formation of an AlN layer on the surface. Moreover, a 1.0- $\mu\text{m}$ -thick AlN diffusion barrier deposited by magnetron sputtering could effectively reduce the diffusion of Fe atoms from a stainless steel foil into a  $\text{Cu}(\text{In,Ga})\text{Se}_2$  film employed in solar cells at 530 °C [19]. AlN as a layer is dense and very stable at high temperatures. But as shown, if deposited as a thin film, it does not allow the formation of a diffusion coating. However, if sufficient AlN can be formed during the aluminizing of a substrate containing sufficient amount of N, the diffusion barrier effect could be achieved by progressive formation of AlN once the coating is formed.

Nitriding is a well-known, mature, and widely employed surface modification process which provides hardness to steels, increasing their wear resistance [20]. Nitriding can be carried out at 480–980 °C by means of  $\text{NH}_3$  [21] or by a  $\text{N}_2$  plasma [22]. Nitriding by means of  $\text{NH}_3$  was employed in this work to enrich the N content of P92 prior to applying an Al slurry and a subsequent heat treatment to induce diffusion. Slurries are suspensions of metal particles in a binder and a solvent which are easily applied by spraying, brushing, or dipping [23, 24]. This method has proven to be economical and practical to produce aluminide coatings both on steels and on Ni base alloys. Using these two surface modification techniques sequentially, a new coating quite different from that obtained by applying the Al slurry under the same conditions, but without prior nitriding, has been obtained. The new coating has been characterized and analyzed by FESEM–EDS and XRD. One of the advantages of this coating application methodology is that it can be used to coat both inner and outer surfaces of heat exchanger tubes employed in steam power plant boilers. The use of coatings allows to retard corrosion caused both from steam and from the combustion gases present in the boiler [16, 25]. Testing of the new coating under steam and oxy-combustion fire-side atmospheres has been carried out and the new coating showed very promising behavior. Comparison of the diffusion behavior at 650 °C of the two coatings with and without prior nitriding also evidenced the diffusion barrier effect.

## Experimental Procedures

### Materials

Sample coupons (20 × 10 × 3 mm) were machined from tubular sections of P92 obtained from Vallourec Mannesmann. The composition is shown in Table 1.

### Coating Application

#### *Nitriding*

Prior to nitriding, the samples surface was ground (Struers P180) in order to remove any impurities present in the substrate that may impede proper nitriding, and then degreased in ethanol in an ultrasonic bath.

Then, nitriding process was carried out by means in a stainless steel chamber at 500 °C for 4 h under flowing  $\text{NH}_3$  at atmospheric pressure. The specimens were hanged during the process so that all faces were nitrided.

**Table 1** P92 composition

	$\text{CO}_2$	$\text{H}_2\text{O}$	$\text{N}_2$	$\text{O}_2$	$\text{SO}_2$
vol%	60	30	7	2	1

### *Slurry Application*

Prior to coating, the samples surface was ground (Struers P40) and degreased in ethanol in an ultrasonic bath. The slurry was produced at INTA by mixing Al powder (5  $\mu\text{m}$ , 99.90 wt% obtained from BendaLutz) with water and a proprietary binder constituted by a mixture of inorganic compounds (without  $\text{Cr}^{+6}$ ). The slurry was homogenized by magnetic stirring prior to spraying with a Sagola spraying gun. Once coated, the samples were left to dry in laboratory air for 3 h. Subsequently, a diffusion heat treatment was performed under argon flow at 700 °C for 10 h. After heat treatment, undiffused slurry residues (“bisque”) were removed by slightly grinding.

### **Characterization**

The as-coated and tested specimens were characterized by light optical microscopy (Leica MEF 4) and field emission scanning electron microscopy (FESEM) employing a JEOL JSM 840 system equipped with an energy-dispersive X-ray spectrometer (EDS) of KEVEX MICROANALYST 8000 with a RÖNTEC signal processor. Phase composition was examined by X-ray diffraction (Philips X'Pert) using the Cu  $K\alpha$  line (0.154 nm).

### **Testing**

#### *Steam Oxidation*

Uncoated substrates were ground (Struers P120) prior to testing. The schematics of the closed loop laboratory rig used at INTA are shown elsewhere [26]. Laboratory air was displaced from the specimen chamber by means of  $\text{N}_2$  which was kept flowing while heating up to the test temperature (approximately at a rate of 600 °C/h). Once the test temperature had been reached, the  $\text{N}_2$  flow was stopped and pure steam was introduced at a linear velocity of 7 cm/s. To carry out weight measurements or to remove samples, the furnace was cooled down to about 300 °C under steam and, before the specimens were removed, the steam flow was replaced by  $\text{N}_2$ . The reheat cycle was also carried out under  $\text{N}_2$  atmosphere up to 650 °C at which point steam was introduced. At least three samples of each type were tested.

#### *Fire-Side Corrosion*

This test was performed using an especially designed experimental rig with four independent lines of  $\text{H}_2\text{O}$ ,  $\text{SO}_2$ ,  $\text{O}_2$ ,  $\text{N}_2$ , and  $\text{CO}_2$  feeding a tubular reactor placed in a furnace shown elsewhere [16]. The gas composition is shown in Table 2. The samples were placed in alumina crucibles and exposed to the flowing gaseous atmosphere at atmospheric pressure and 650 °C. The exhaust gas was neutralized by bubbling it through alkaline solutions. The test began by flowing nitrogen for 1 h while the furnace was heating up to the test temperature. Then, the nitrogen line was closed and the corrosive gases and water vapor were introduced at a linear velocity

**Table 2** Composition of the oxyfuel model atmosphere for the fire-side corrosion test

	Fe	Cr	N	Ni	Si	V	S	Mo	C	Mn	W
wt%	Bal.	8.800	0.046	0.060	0.030	0.200	0.006	0.400	0.100	0.500	1.800

of 3 cm/s. Every 7 days the test was stopped to weight the specimens by cutting the corrosive gas mixture and turning the furnace off and introducing  $N_2$ . After approximately 2 h once the temperature was 300 °C or lower the samples were removed. At least three samples of each type were tested.

## Results and Discussion

### Coating generation and Characterization

After nitriding P92 at 500 °C with  $NH_3$ , a depth of  $\approx 30 \mu m$  was enriched in nitrogen, as shown in Fig. 1. Nitrogen mainly accumulated within the grain boundaries (5 wt% in average) which were also rich in Cr. Some needle-like features were also visible within the grains. Nitrogen was also detected in the grain's bulk by EDS (1 wt%). According to Blawert et al. [27], the amount of N that can be kept in solution in the substrate depends on the Cr content, the higher the Cr the higher the N solubility. At high N contents, both  $\epsilon-Fe_{2-3}N$  and CrN can be formed. The XRD pattern of the samples exhibits low intensity peaks that can be attributed to  $Fe_2N$  and CrN. Rather than a continuous nitride layer, on the surface of the specimen, an oxide rich in Fe, Cr, and N could be observed. The formation of such a continuous nitride film depends on the temperature and the Cr content of the steel among other factors [27].

After removing (by grinding) the surface oxide of the nitrided specimens, an Al slurry was applied by spraying, followed by a diffusion heat treatment at 700 °C. Surprisingly, an overlay coating consisting of an Al-rich layer containing Cr and Fe was obtained (Fig. 2a). This new 20–30  $\mu m$  coating was quite different from that obtained by applying the Al slurry under the same conditions, but without prior nitriding, which is thicker ( $\approx 80 \mu m$ ) and composed of the intermetallic phases

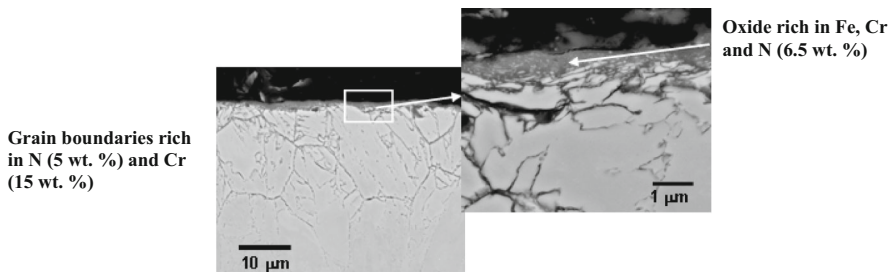


**Fig. 1** FESEM image of P92 nitrided at 500 °C for 4 h

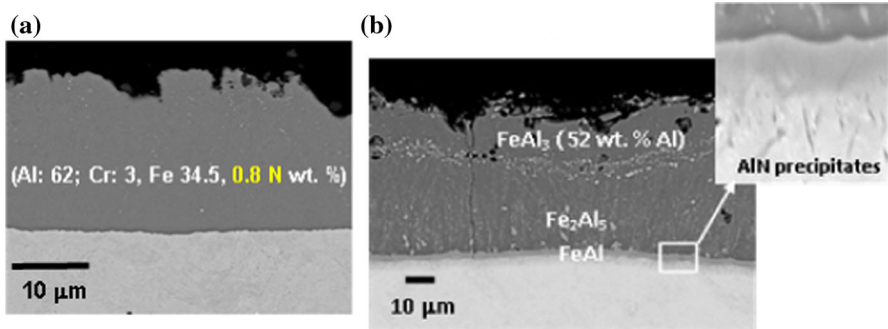


**Fig. 2** FESEM image of: **a** aluminized and heat-treated (10 h at 700 °C) previously nitrated P92 and **b** aluminized and heat-treated (10 h at 700 °C) P92

FeAl<sub>3</sub>, Fe<sub>2</sub>Al<sub>5</sub>, and FeAl as shown in Fig. 2b [7]. Moreover, the acicular AlN precipitates that formed within the substrate were absent in the new coating, in which there was a clear interface with the substrate. The absence of Al in the substrate was confirmed by EDS point analysis carried out immediately beneath the coating–substrate interface. Another important difference was the absence of thickness-through cracks which developed on the intermetallic coating (Fig. 2b), likely due to thermal expansion coefficients mismatch between the different intermetallic phases and the substrate, as well as to the brittleness of the Fe<sub>2</sub>Al<sub>5</sub> phase.

The coating phase composition was determined by XRD (Fig. 3a). The highest intensity peaks correspond to Al, and other lower intensity peaks could be attributed to FeAl<sub>3</sub> and to Al<sub>13</sub>Cr<sub>2</sub>. This indicates that the coating was mostly composed of an Al solid solution with Fe and Cr. Very few and small precipitates rich in Cr could be seen in a high-magnification image of the coating which could correspond to Al<sub>13</sub>Cr<sub>2</sub> (Fig. 4). To the best of our knowledge, there is no precedent of an Al solid solution coating. The Fe content measured by EDS (34.5 wt%) corresponds indeed to an Al solid solution mixed with FeAl<sub>3</sub> according to the Al–Fe phase diagram

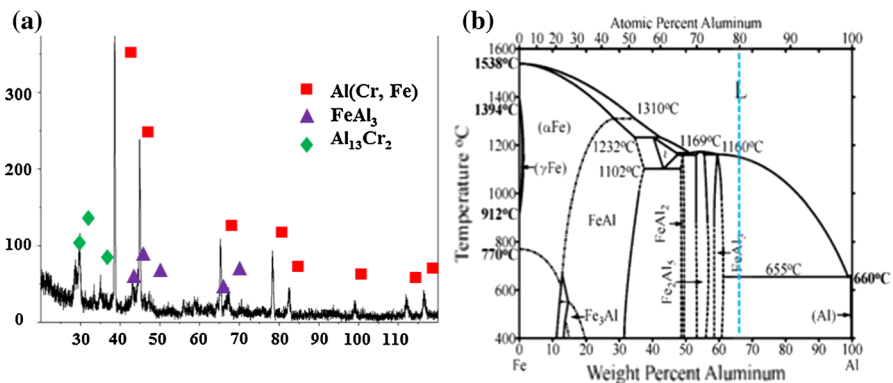


**Fig. 3** **a** XRD pattern of the new NITRAL coating and **b** Al–Fe phase diagram [28]

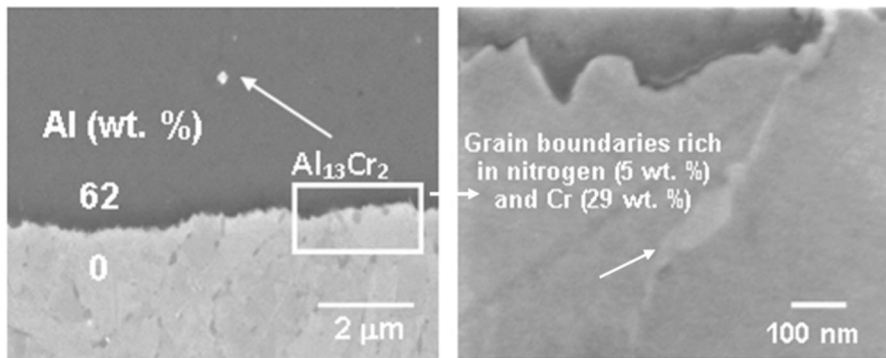


**Fig. 4** High-magnification FESEM images of the coating–substrate interface of aluminized and heat-treated NITRAL coating on P92

shown in Fig. 4b [28]. The new nitrided-aluminide coating (NITRAL for short) is meant to be used in steam power plants at a maximum temperature of 650 °C.  $\text{FeAl}_3$  cannot be differentiated as a separate phase by high-magnification FESEM but must be present as shown by the DRX pattern. No peaks corresponding to nitrides that could be present in the coating were observed. Moreover, in the coating–substrate interface, no features were observed, indicating that a nitride continuous layer formed under the present conditions.

The formation of an Fe aluminide coating on steels, by applying a slurry and heat treating at 700 °C, is thought to take place by a very fast sequence of steps: (1) melting of Al, (2) immediate dissolution of the substrate in molten Al, (3) liquid–solid diffusion, (4) solidification of intermetallic high melting point phases, and (5) interdiffusion between the new intermetallic phases and the substrate [29]. The results obtained in this work employing previously nitrided P92, first evidenced that before solidification, the amounts of Fe and Cr that have dissolved in molten Al, were not high enough to generate the Fe richer intermetallic phases present in the reference aluminide coating. Moreover, once the coating has solidified, further coating–substrate interdiffusion was hindered by the presence of N, both in the substrate and in the coating. Nitrogen was mostly concentrated in the substrate grain boundaries, likely hindering both Fe outward- and Al inward-diffusion. The presence of N within the grain may also hinder bulk diffusion.

### Corrosion Testing

The two coatings were tested together for comparison purposes under steam and a laboratory oxyfuel atmosphere ( $\text{CO}_2$ : 60;  $\text{N}_2$ : 7;  $\text{O}_2$ : 1;  $\text{H}_2\text{O}$ : 30;  $\text{SO}_2$ : 1 in vol%) at 650 °C, showing in both cases excellent protective behavior up to at least 2000 h. Figure 5 shows for instance the mass variation after exposure to the laboratory oxyfuel atmosphere of uncoated and coated P92 specimens, coatings being both the reference aluminide without nitriding and the new NITRAL. However, the uncoated substrate experienced an important weight gain; the two types of coated specimens underwent very little increase in weight up to at least 2000 h. The mass variation of

the coated specimens exposed to steam was quite similar (not shown due to space limitation).

After 2000 h of exposure to the oxyfuel atmosphere at 650 °C, uncoated P92 developed a multilayered, approximately 200 μm oxide scale, exhibiting hematite ( $\text{Fe}_2\text{O}_3$ ) on top of magnetite ( $\text{Fe}_3\text{O}_4$ ) and finally a mixture of magnetite and Fe–Cr spinel [ $(\text{Fe}, \text{Cr})_3\text{O}_4$ ] [26]. This oxide also contained sulfur, mostly within the Fe–Cr spinel.

In contrast, very thin  $\text{Al}_2\text{O}_3$  formed on the reference and on the NITRAL coatings, which protected the substrate preventing its degradation. The microstructure of both types of coatings as function of exposure time is shown in Fig. 6. It can be clearly seen that the diffusion behavior of the two coatings was quite different. As mentioned in the introduction, the reference aluminide coating exhibits significant microstructural and composition changes due to interdiffusion. The Al richer phases ( $\text{FeAl}_3$  and  $\text{Fe}_2\text{Al}_5$ ) transform to FeAl, which growth in thickness from 4–5 to 40–45 μm after 2000 h. Moreover, AlN precipitates deeper within the substrate, indicating that its N content has been reduced and therefore its strengthening effect diminished. In addition, the through-thickness cracks originally

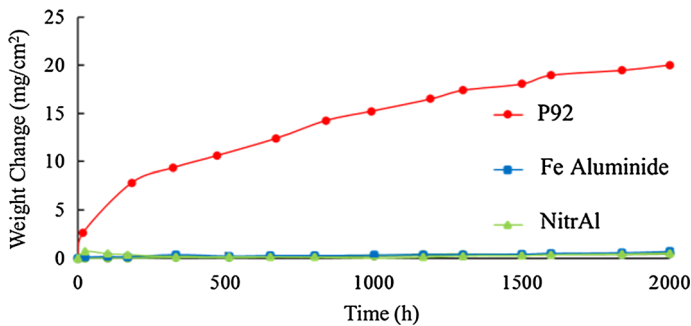


**Fig. 5** Mass variation of P92, uncoated and coated with both the reference aluminide and the new NITRAL coating after exposure to a laboratory oxyfuel atmosphere (Table 2) at 650 °C

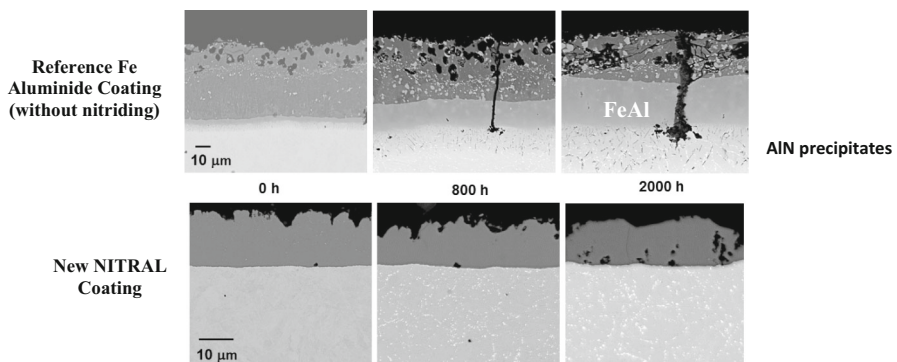


**Fig. 6** FESEM images of the reference Fe aluminide and NITRAL coatings exposed to an oxycombustion atmosphere at 650 °C as a function of exposure time



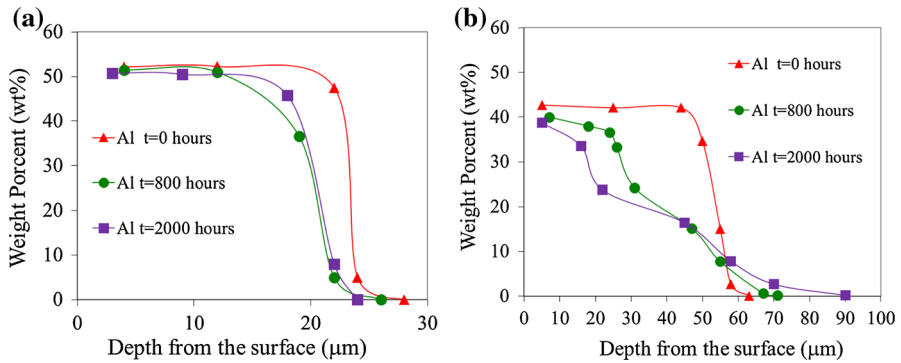


**Fig. 7** Element profiles of the new NITRAL (a) and the reference aluminide (b) coatings as function of time at 650 °C

present in the coating have widened, although no attack was observed, even at the bottom of the crack, where the substrate has been reached. The crack surfaces were likely covered by protective  $\text{Al}_2\text{O}_3$  [6]. Besides, the NITRAL coating did not interact with the substrate and maintained the same overlay microstructure of the “as deposited” layer. The main difference observed on the exposed samples was the aging of the substrate characterized by the precipitation of the Laves phase ( $\text{Fe}_2\text{W}$ ), typical of ferritic steels exposed to 650 °C for long times [30]. No Al could be measured (by EDS) within the substrate, in the area immediately in contact with the coating. The thickness and Al content of the coating remained similar as it is shown in Fig. 7, where the concentration profile as a function of exposure time is shown for both coatings. However, some differences were observed which were attributed to experimental variations, for instance the thickness of the initial samples.

After 2000 h, the surface Al content of the reference aluminide was still high, but past work has shown how, on increasing exposure time, it continuously decreases, reaching 7 wt% after 70,000 h [31]. This may seem as a very long time, but coatings are expected to last 300,000 h in steam power plants. On the other hand, the new coating seems quite stable although longer exposure experiments are necessary.

## Conclusions

A new overlay, Al solid solution coating containing Fe, Cr, and N has been deposited on P92 by a three-step process consisting of: (1) nitriding by means of  $\text{NH}_3$  at 550 °C for 4 h, (2) applying a Cr VI free water-based Al slurry by means of spraying, and (3) heat treating at 700 °C for 10 h. Once the coating was formed, likely by substrate dissolution on molten Al followed by rapid solidification, no coating–substrate interdiffusion was observed at 650 °C up to at least 2000 h. Nitrogen present mainly in the substrate grain boundaries seems to hinder both inward Al- and outward Fe-diffusion. The coating protects ferritic steels from steam and oxyfuel fire-side corrosion at temperatures not exceeding 650 °C.

**Acknowledgements** The authors are grateful for the support by the Spanish Ministry of Economy and Competitiveness for financial support (ENE2014-52359-C3-1-R) as well as the EC (POEMA, G.A. No.: 310436). The authors also acknowledge all members of the Metallic Materials Area at INTA for technical support, as well as Cristina Gallego and Luis Angurel from the “Consejo Superior de Investigaciones Científicas”(CSIC)—Zaragoza for their excellent microscopy work.

## References

1. R. Sakidja, J. H. Perepezko and P. Calhoun, *Oxidation of Metals* **81**, 167 (2014).
2. S. C. Deevi and V. K. Sikka, *Progress in Material Science* **42**, 177 (1997).
3. J. W. Lee and Y. C. Kuo, *Surface & Coating Technologies* **200**, 1225 (2005).
4. H. Lee, H. Kang, J. Kim, H. K. Shin, J. Lee, S. H. Huh, J. Sung and H. J. Lee, *Surface & Coating Technologies* **240**, 221 (2014).
5. L. Meifeng, L. Lei, W. Yating, Z. Cheng, W. Wenbin and P. Deng, *Journal of Alloys and Compounds* **551**, 389 (2013).
6. A. Agüero, K. Spiradek, M. Gutiérrez, R. Muelas and S. Höfner, *Materials Forum* **595–598**, 251 (2008).
7. S. Velraj, Y. Zhang, E. W. Hawkins and B. A. Pint, *Materials and Corrosion* **63**, 909 (2010).
8. O. Knotek, E. Lugscheider, F. Löffler and W. Beele, *Surface & Coating Technologies* **68/69**, 22 (1994).
9. J. Mueller and D. Neuschuetz, *Vacuum* **71**, 247 (2003).
10. T. Narita, F. Land, K. Z. Thosin, T. Yoshioka, T. Izumi, H. Yakuwa and S. Hayashi, *Oxidation of Metals* **68**, 343 (2007).
11. F. Wu, H. Murakami and A. Suzuki, *Surface & Coating Technologies* **168**, 62 (2003).
12. J. A. Haynes, Y. Zhang, K. M. Cooley, L. Walker, K. S. Reeves and B. A. Pint, *Surface & Coating Technologies* **188–189**, 153 (2004).
13. X. Tan, X. Peng and F. Wang, *Surface & Coating Technologies* **274**, 62 (2013).
14. Z. Xua, R. Muc, L. Hec and X. Caoa, *Journal of Alloys and Compounds* **466**, 471 (2008).
15. A. Agüero, V. González, M. Gutiérrez, R. Knödler, R. Muelas and S. Straub, *Materials and Corrosion* **62**, 561 (2011).
16. A. Agüero, I. Baraibar, V. González, R. Muelas and D. Plana, *Oxidation of Metals* **85**, 263–281 (2016).
17. Y. Y. Chang, C. C. Tsaun and J. C. Rock, *Surface & Coating Technologies* **200**, 5688 (2006).
18. A. Rouaix-Vande Put and B. Pint, *Surface & Coating Technologies* **206**, 5036 (2012).
19. B. Li, J. Li, L. Wu, W. Lin, Y. Sun and Y. Zhang, *Journal of Alloys and Compounds* **627**, 1 (2015).
20. Web site: [http://www.asminternational.org/documents/10192/1849770/06950G\\_Chapter\\_1.pdf](http://www.asminternational.org/documents/10192/1849770/06950G_Chapter_1.pdf). Accessed 10 March 2016.
21. E. J. Mittemeijer and M. A. J. Somers, *Surface Engineering* **13**, 483 (1997).
22. S. D. Oliveira, A. P. Tschiptschin and C. E. Pinedo, *Materials & Design* **28**, 1714 (2007).
23. A. Agüero, M. Gutiérrez and V. González, *Materials at High Temperature* **27**, 257 (2008).
24. B. Rannou, B. Bouchaud, J. Balmain, G. Bonnet and F. Pedraza, *Oxidation of Metals* **81**, 139 (2014).
25. A. Agüero, *Energy Materials* **3**, 35 (2008).
26. A. Agüero, V. González, M. Gutiérrez and R. Muelas, *Surface & Coating Technologies* **237**, 30 (2013).
27. C. Blawert, B. L. Mordike, U. Rensch, G. Schreiber and H. Oettel, *Surface Engineering* **18**, 249 (2002).
28. U. R. Kattner, Al–Fe (Aluminum–Iron). in *Binary Alloys Phase Diagrams*, Vol. 1, eds. T. B. Massalski et al. (ASM International, USA, 2001), pp. 147–149.
29. A. Agüero, M. Gutiérrez and V. González, *Defect and Diffusion Journal* **289–292**, 243 (2009).
30. L. Korcakova, J. Hald and M. A. J. Somers, *Materials Characterization* **47**, 111 (2001).
31. A. Agüero, M. Gutiérrez, R. Muelas and K. Spiradek-Hahn, *Surface Engineering* (2016). doi:10.1080/02670844.2016.1155691.